

Phase Retrieval Problem. Application to VLBI Mapping of Active Galactic Nuclei

A.T. Bajkova

Pulkovo Astronomical Observatory, Russian Academy of Sciences, St.-Petersburg, Russia

Abstract—The well-known phase problem which means image reconstruction from only spectrum magnitude without using any spectrum phase information is considered basically in application to VLBI mapping of compact extragalactic radio sources (active galactic nuclei). The method proposed for phaseless mapping is based on the reconstruction of the spectrum magnitude on the entire UV plane from the measured visibility magnitude on a limited set of points and the reconstruction of the sought-for image of the source by Fienup's error-reduction iterative algorithm from the spectrum magnitude reconstructed at the first stage. It is shown that the technique used ensures unique solution (within a class of equivalent functions) for AGNs with typical structure morphology "bright core + weak jet". The method proposed can be used, for example, for imaging with ultra-high resolution using a space-ground radio interferometer with a space antenna in a very high orbit ("RadioAstron"). In this case, a multi-element interferometer essentially degenerates into a two-element interferometer and the degeneracy of the close-phase relations prevents the use of standard methods for hybrid mapping and self-calibration. The capabilities and restrictions of the method are demonstrated on a number of model experiments. For a few selected AGNs the images are obtained from VLBA observations.

1 Introduction to phase retrieval problem

In this paper we consider the problem of image reconstruction from only spectral magnitude when spectral phase of an object is totally unknown.

Why this problem is important? In general case, as was shown by many authors, phase information is more important than magnitude information, because phase information is responsible for positions of details of image. Importance of spectral phase is clear from Fig.1. In Fig.1(a) the picture of a man is shown. The image (b), reconstructed using original Fourier spectrum phase information of the model image and uniform spectral magnitude allows us to recognize the features of the portrait. The image (c) reconstructed from original spectral magnitude and zero-valued spectral phase does not give anything common with original portrait (a).

Let us formulate the phase problem in discrete form. Let the discretization in spatial and spectrum domains of an object be fulfilled in accordance with Kotelnikov-Shannon theorem and size of two-dimensional maps be equal to $N \times N$ samples.

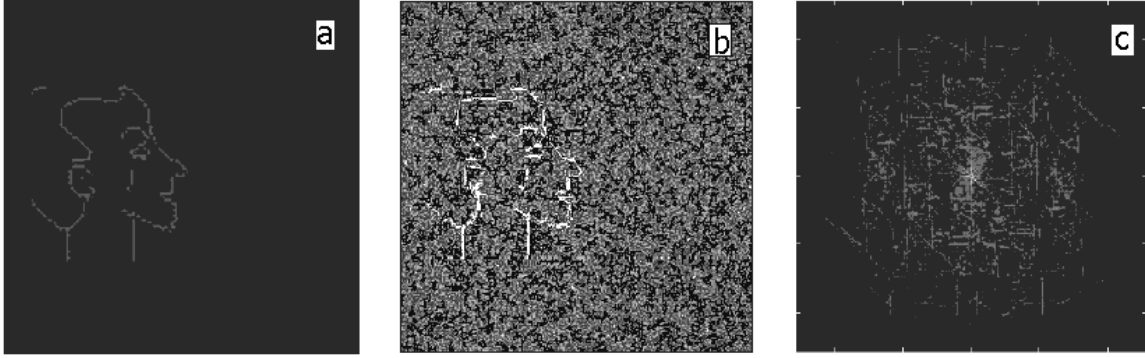


Figure 1: Importance of phase: (a)model: all nonzero points=1, (b) corresponding image with original spectral phase and uniform spectral magnitude, (c)corresponding image with original spectral magnitude and zero-valued spectral phase

Spectrum of an object is calculated as discrete two-dimensional Fourier transform of two-dimensional sequence $x_{ml}, m, l = 0, \dots, N$ as follows:

$$X_{nk} = \frac{1}{N} \sum_{m=0}^{N-1} \sum_{l=0}^{N-1} x_{ml} \exp(-\frac{j2\pi}{n}(nm + kl)) = A_{nk} + jB_{nk} = M_{nk} \exp(j\Phi_{nk}), \quad (1)$$

where $n, k = 1, \dots, N$, A_{nk}, B_{nk}, M_{nk} and Φ_{nk} are real part, imaginary part, magnitude and phase of spectrum correspondingly.

We consider the case of image formation systems when data are delivered not directly on an object but on its Fourier spectrum. If data are complete, i.e. we have both magnitude and phase of spectrum, then the image sought-for can be obtained by simple inverse Fourier transform of data:

$$x_{ml} = \frac{1}{N} \sum_{n=0}^{N-1} \sum_{k=0}^{N-1} M_{nk} \exp(j\Phi_{nk}) \exp(\frac{j2\pi}{n}(nm + kl)), \quad (2)$$

But if the data are not complete, i.e. we have information only about magnitude or only about phase of the spectrum, the problem of retrieval of missing information arises, because only presence of both components gives correct representation of an object. Here we consider a typical for many fields problem of phase or, equivalently, image x_{ml} retrieval from its Fourier spectrum magnitude M_{nk} . Such a problem is called "phase problem". The most significant works devoted to phase problem are published by Gerchberg and Saxton (1972), Fienup (1978, 1982, 1983), Fienup, Crimmins and Holsztynski (1982), Fienup et al (2006, 2009), Huang, Bruck and Sodin (1979), Hayes (1982), Oppenheim and Lim (1981), Dainty and Fiddy (1984), Sanz and Huang (1983).

2 The uniqueness of the solution

In the most general formulation where constraints are imposed only on the spectrum magnitude, the problem of reconstructing the function has an infinite set of solutions. Indeed, any function that has a given spectrum magnitude and an arbitrary spectral phase satisfies these constraints, and, if at least one solution is known, the other can be obtained by convolving this solution with a function that has an arbitrary phase and a spectrum magnitude equal to unity at all frequencies.

However, a significant narrowing of the set of solutions is possible for certain constraints imposed on the function being reconstructed in the spatial domain (Stark 1987). One of these is the constraint imposed on the spatial extent of an object; i.e., the sought-for function must have a finite carrier. Another severe constraint in the spatial domain is the requirement of real valuedness and nonnegativity. Below, in solving the phase retrieval problem, we assume that the sought-for function satisfies these constraints; i.e., it is real and nonnegative and has a finite extent. Further we always will assume that sought-for solution to x_{ml} is non-negative and has rectangular support $R(m, l) : m = M_1, \dots, M_2, l = L_1, \dots, L_2$, where $|M_2 - M_1| \leq N/2, |L_2 - L_1| \leq N/2$ in order to compute spectrum modulus without aliasing.

The finite extent of an object (the finiteness of the function) ensures that the Fourier spectrum is analytic in accordance with the Wiener-Paley theorem (Khurgin and Yakovlev 1971). As a result, this spectrum can be reconstructed from the known part of it, which is used to reconstruct images from the visibility function measured on a limited set of points in the UV plane.

If we determine the class of equivalent functions to within a linear shift and reversal of the argument (rotation through 180°), then all of the functions that belong to this class have the same spectrum magnitude. The solution of the phase retrieval problem is assumed to be unique if it was determined to within the class of equivalent functions.

In the case of one-dimensional functions, even these severe constraints on finiteness and nonnegativity do not guarantee a unique reconstruction from the spectrum magnitude. As the dimensionality of the function increases ($n \geq 2$), a unique (to within the class of equivalent functions) solution becomes possible, except for the degenerate cases defined on the set of measure zero (Bruck and Sodin 1979; Hayes 1982). This follows from the qualitative difference between the properties of the z -transformations of one-dimensional and multidimensional sequences.

For a unique solution to exist, the z -transformation must be irreducible, which is not achievable in principle in the one-dimensional case and almost always holds in the multidimensional case. Since we deal with two-dimensional images in VLBI, we assume that the solution of the phase retrieval problem exists and is unique. However, the existence of a unique solution does not yet guarantee that the retrieval algorithms converge. The papers by Gerchberg and Saxton (1972) and Fienup (1978) are of greatest importance in developing the theory and algorithms of solving the phase retrieval problem.

3 Fienup's error-reduction phase retrieval algorithm

Here we consider one of the most efficient algorithm for image reconstruction from the spectrum magnitude of an object, proposed by Fienup, so called error-reduction algorithm.

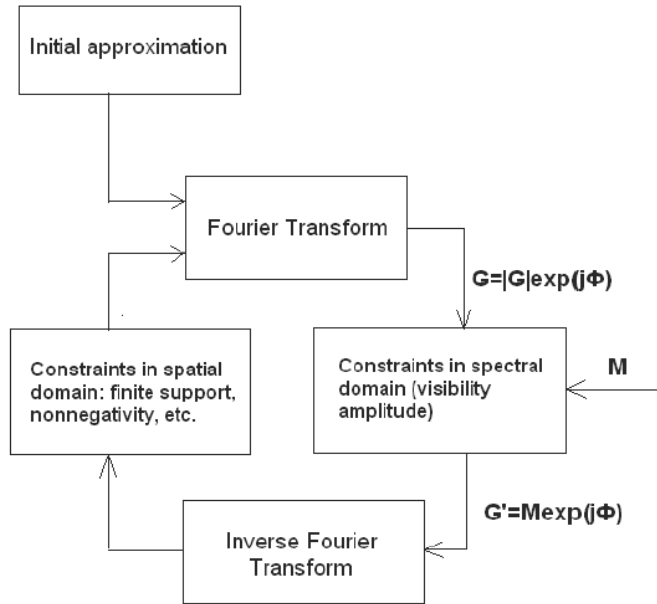


Figure 2: Fienup's error-reduction phase retrieval algorithm

Recall that Fienup's error-reduction algorithm (Fig.2) is an iterative process of the passage from the spatial domain of an object to the spatial frequency domain and back (using the direct and inverse Fourier transforms) in an effort to use the input constraints on the spectrum magnitude of the object in the frequency domain and the constraints on its nonnegativity and finite extent in the spatial domain. The finite carrier within which the source is expected to be localized should be specified in the form of a rectangle. Fienup et al.(1982) estimated the size of the carrier from the autocorrelation function equal to the inverse Fourier transform of the square of the spectrum magnitude for the object. Very important advantages of Fienup's algorithm are its high stability against noise (Sanz and Huang 1983) (stability means that a small change in input data causes the solution to change only slightly) and high speed (due to the application of fast Fourier transform algorithms) compared to other algorithms.

In practice, the error-reduction algorithm usually decreases the error rapidly for the first few iterations but much more slowly for later iterations. In all our further experiments we used 100 iterations. But this algorithm does not guarantee conversion to the true solution having stagnation problem and depending on the initial approximation. The problem of convergence is hard particular in case of complicated images. One of examples of stagnation is shown in Fig.3, from which we can see that phase retrieval algorithm did not give true solution. Note that in all experiments dealing with the Fienup's error-reduction algorithm we used δ -function as an initial approximation.

4 The role of a reference point

In this section we demonstrate the essential role of a reference point, which may be introduced into the image. As it is seen from Fig.3, in case of absence of some dominated

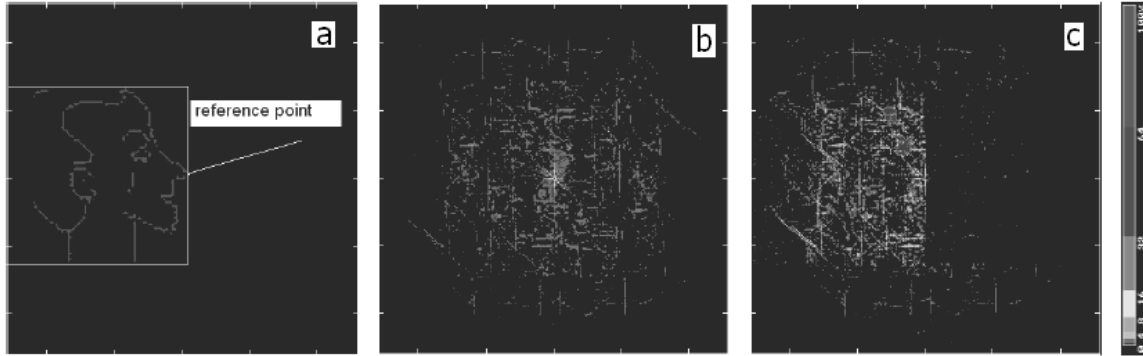


Figure 3: Image reconstruction result for an object without dominating reference point: (a) model: all nonzero points=1, reference point is located at the edge of object, reference point value=1, rectangular boundaries of the object are given in white color, (b) corresponding image with original spectral amplitude and zero-valued spectral phase, (c) Fienup's algorithm output image

point in the object the phase retrieval algorithm can fail. Fig.4 shows results of phase retrieval for different values of the reference point which is located at the edge of the image as it is shown in Fig.3 (a). We can see from Fig.4 that the increase of the reference point value leads to improving the reconstruction quality. With increase of the reference point value the structure of the object becomes more and more apparent in the images shown in the left column of Fig.4, which are obtained using inverse Fourier transform from original spectral magnitude and zero-valued spectral phase. We can conclude that spectral magnitude contains more information on spectral phase for images with higher reference point values. Therefore Fienup's error-reduction algorithm for such images works much better ensuring unique true solution. Location of a reference point may be arbitrary: outside, at the edge or inside of image. In Fig.5 the case of location of the reference point inside of image is shown.

5 Application of Fienup's error-reduction algorithm to imaging AGNs

Above we established that presence in the image of a strong dominated point leads to unique solution of phase retrieval problem. Most of extragalactic radio sources (active galactic nuclei) characterizing by structure morphology "bright compact core + weak jet" meet this requirement. Results of modelling of phase retrieval problem for a few sources with different positions and amplitudes of gaussian components are shown in Fig.6. We can see that images obtained from original spectral magnitude and zero-valued spectral phase (column(c)) contain information about real structure (equivalently spectral phase) of an object. Output images of Fienup's phase retrieval algorithm visually do not differ from model images shown in column (a). In all considered cases compact core of sources (at the center of maps) strongly dominate over other components. In case of less dominating of core the result of reconstruction is much worse, as it is demonstrated in Fig.7.

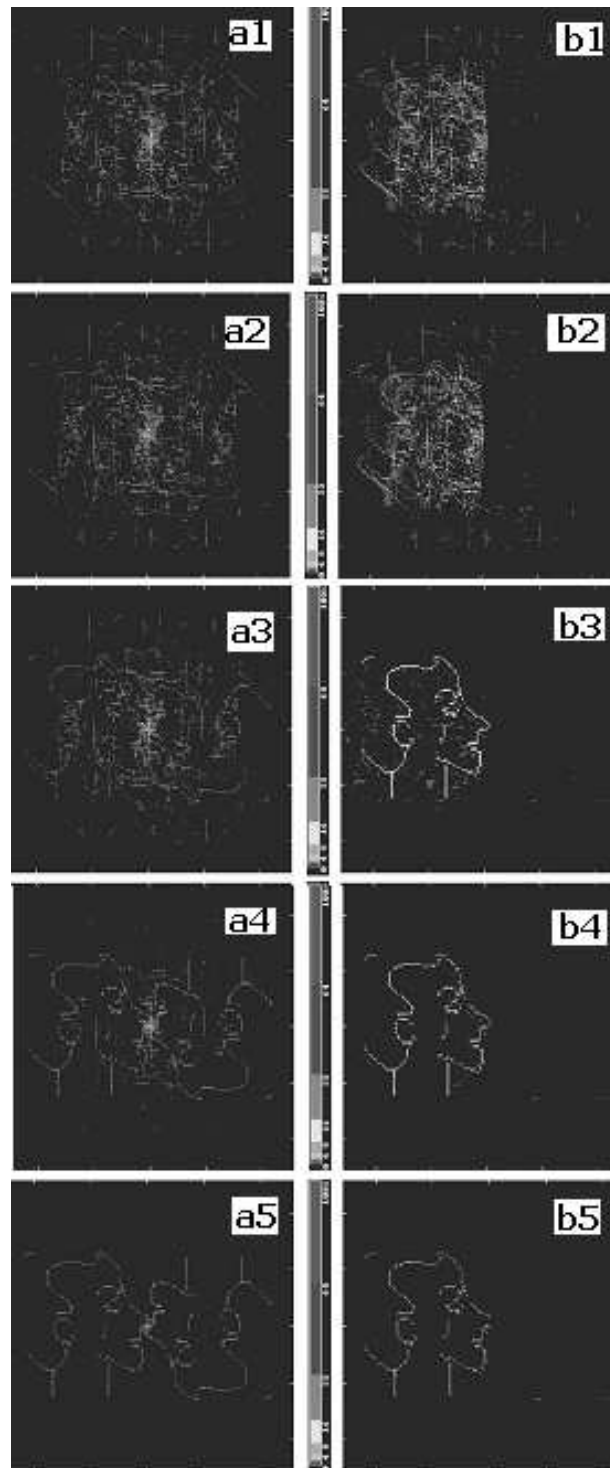


Figure 4: Reconstruction quality for images with different reference point values (the reference point is located at the edge of the image): left column (a):images with original spectrum magnitude and zero-valued spectrum phase, right column (b): Fienup's algorithm output images; (a1,b1): reference point value=2, (a2,b2): reference point value=5, (a3,b3): reference point value=10, (a4,b4): reference point value=20, (a5,b5): reference point value=50

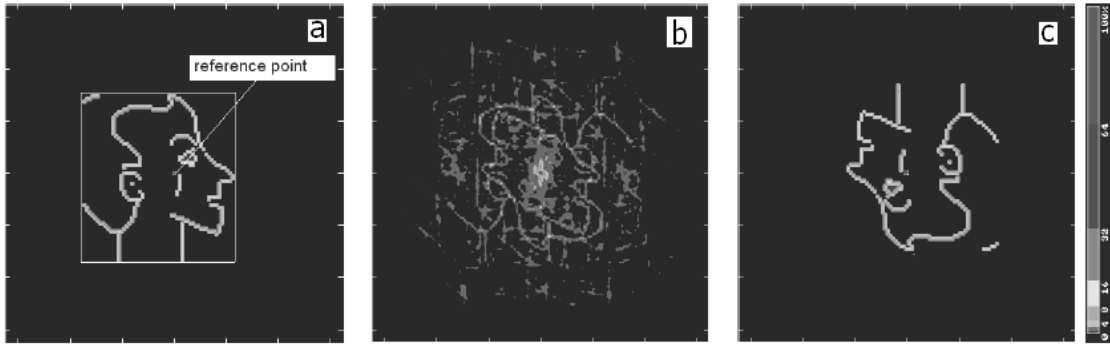


Figure 5: A reference point is located inside of the image: (a) model: all nonzero points=1, reference point value=20, (b)corresponding image with original spectral amplitude and zero-valued spectral phase, (c) Fienup’s algorithm output image

So, requirement of strong dominating of compact core over more weak components of the source is very important for reliable phase retrieval (equivalently image reconstruction) from only spectral magnitude. Fortunately, practically all AGNs meet this requirement.

6 ”Phaseless” mapping in VLBI

The algorithms for image reconstruction from the spectral magnitude of an object, the most efficient of which are Fienup’s algorithm and its various modifications, require knowledge of the entire input two-dimensional sequence of sampled points. In VLBI, however, the visibility function is measured only on a limited set of points in the UV plane, revealing large unfilled areas and a diffraction-limited constraint. Therefore, prior reconstruction of the visibility magnitude on the entire UV plane from a limited data set is required to successfully use existing reconstruction algorithms like Fienup’s algorithm.

Thus, the suggested phaseless aperture synthesis method consists of the following steps: (1) prior reconstruction of the visibility magnitude (the object’s spectrum) on the entire UV plane, and (2) reconstruction of the sought-for image using Fienup’s algorithm or its modifications (Fienup 1978, 1982; Bajkova 2004, 2005) from the spectrum magnitude reconstructed at the first step of the method. The first step is performed through the reconstruction of an intermediate image that satisfies the measured visibility magnitude and a zero phase. Clearly, the intermediate image is symmetric relative to the phase center of the map. The Fourier transform of the image obtained yields the spectrum magnitude of the source extrapolated to the region of the UV plane where there are no measurements.

The intermediate image can be reconstructed from the visibility magnitude by the standard method of analytic continuation of the spectrum using the non-linear CLEAN deconvolution procedures or the maximum entropy method (MEM) (Cornwell et al. 1999). Therefore, an important requirement for the visibility magnitude is its analyticity. As we noted in the previous section, this condition is satisfied for most of the compact extragalactic radio sources if the flux from the central compact component dominates over the flux from the remaining fainter components.

Note an important point concerning the use of the maximum entropy method. In

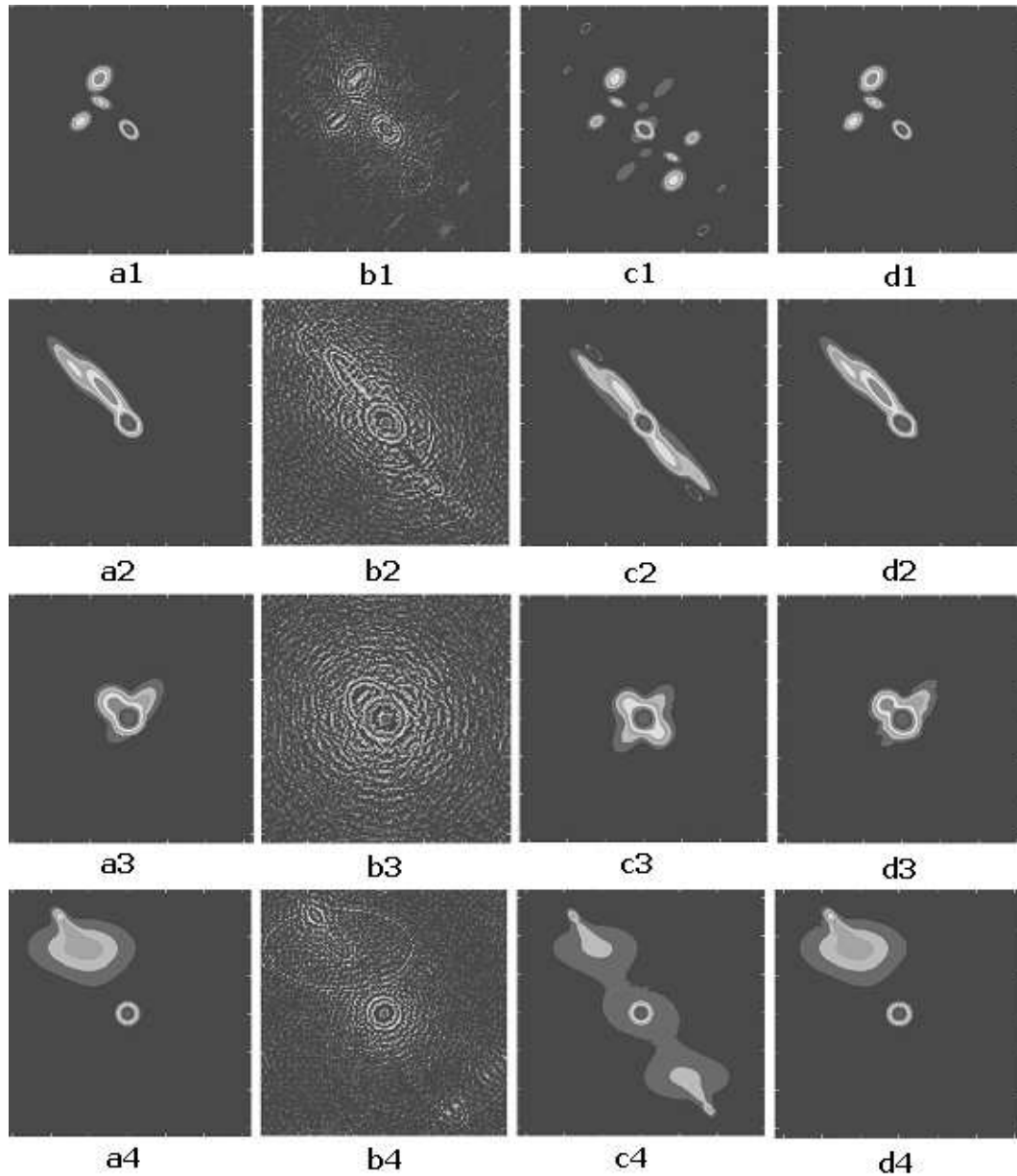


Figure 6: Modelling of the phase retrieval procedure for compact sources with different morphology: columns: (a): models, (b): images with original spectral phase and uniform spectral magnitude, c): images with original spectral magnitude and zero-valued spectral phase, (d): Fienup's algorithm output images; rows: (1) source-1, (2) source-2, (3) source-3, (4) source-4

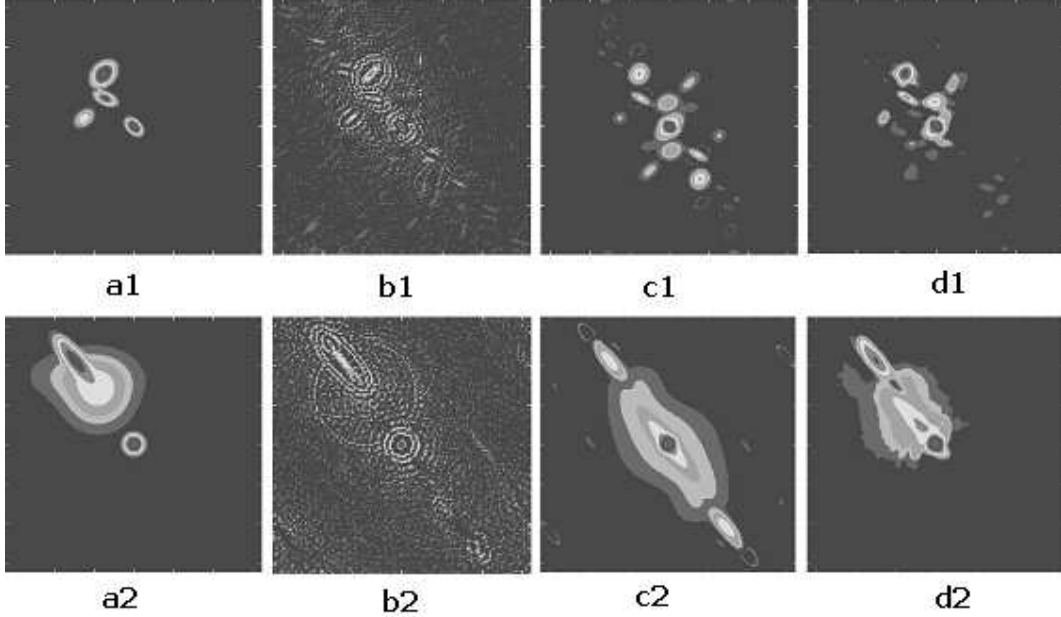


Figure 7: Modelling of the phase retrieval procedure for AGNs with two comparable bright components: columns: (a): models, (b): images with original spectral phase and uniform spectral magnitude, c): images with original spectral magnitude and zero-valued spectrum phase, (d): Fienup's algorithm output images; rows: (1) source-5, (2) source-6

contrast to the CLEAN method: the solution based on the standard MEM is strictly positive, while the sought-for intermediate image with a zero spectral phase is generally alternating, taking on both positive and negative values.

For reconstruction of images of real sign-variable and complex functions the generalized maximum entropy method has been developed by Baikova (1992) (see also Frieden, Bajkova (1994)). This method is implemented in the Pulkovo VLBI data reduction software package VLBIImager.

Note also that because the GMEM is designed for the reconstruction of sign-variable functions, it allows one to obtain unbiased solutions. The bias of the solution is one of the problems of the conventional MEM (Cornwell et al. 1999), which may lead to a substantial nonlinear distortion of the final image if the data contain errors.

For the GMEM, the Shannon-entropy functional has the form

$$E(\alpha) = - \int (x^p(t) \ln(\alpha x^p(t)) + x^n(t) \ln(\alpha x^n(t))) dt, \quad (3)$$

$$x^p(t) > 0, x^n(t) > 0, \quad (4)$$

where $x^p(t)$ and $x^n(t)$ are the positive and negative components of the sought-for image $x(t)$ (Fig.8), i.e. the equation $x(t) = x^p(t) - x^n(t)$ holds. $\alpha \neq 0$ is a parameter responsible for the accuracy of the separation of the negative and positive components of the solution $x(t)$, and therefore critical for the resulting image fidelity.

It is easy to show (Baikova 1992) that solutions for $x^p(t)$ and $x^n(t)$ obtained with the Lagrange optimization method are connected by the expression $x^p(t) \times x^n(t) = \exp(-2 - 2 \ln \alpha) = K(\alpha)$, which depends only on the parameter α . This parameter is responsible for dividing the positive and negative parts of the solution: the larger α is, the more accurate

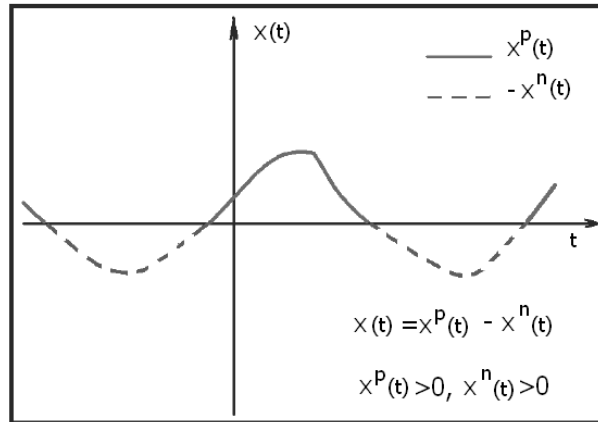


Figure 8: Form of Generalized MEM solution

is the discrimination. On the other hand, the value of α is constrained by computational limitations.

Results of modelling of "phaseless" VLBI mapping using the GMEM and Fienup's phase retrieval algorithm for three model sources are shown in Fig.9. As can be seen, the results obtained are of quite satisfactory quality. It is necessary to note, that solution of the phase problem in case of incomplete magnitude data significantly depend on accuracy of GMEM intermediate images. Result of the GMEM reconstruction depends on quality of data. We investigated quality of imaging for typical level of additive noise and different level of amplitude errors in visibility data. Results are shown in Fig.10. We can see that the reconstruction method is very stable to errors in data and even in the case of large amplitude errors we have output images which adequately reflect basic features of the source.

The proposed technique was used for mapping seven selected AGNs characterized by complicated structure of jets. We used VLBA data from NRAO archive. Corresponding UV coverages, intermediate GMEM images and final images obtained using Fienup's phase retrieval procedure are shown in Fig.11-17. These Figures contain all basic information on both input data and images obtained. We can see, that all intermediate images contain true information about structure of jets what led to easy reconstruction of spectral phase of sources on the final stage of reconstruction using Fienup's algorithm. The images obtained are in good agreement with ones published in literature what indicates high reliability of our approach for VLBI imaging.

7 Modelling of "phaseless" mapping for "RadioAstron" mission

Here we consider the problem of mapping with ultra-high angular resolution using a space-ground radio interferometer with a space antenna in a high orbit, whose apogee height exceeds the radius of the Earth by a factor of tens. "RadioAstron" mission (Kardashev 1997) represents such a system. Its basic param-

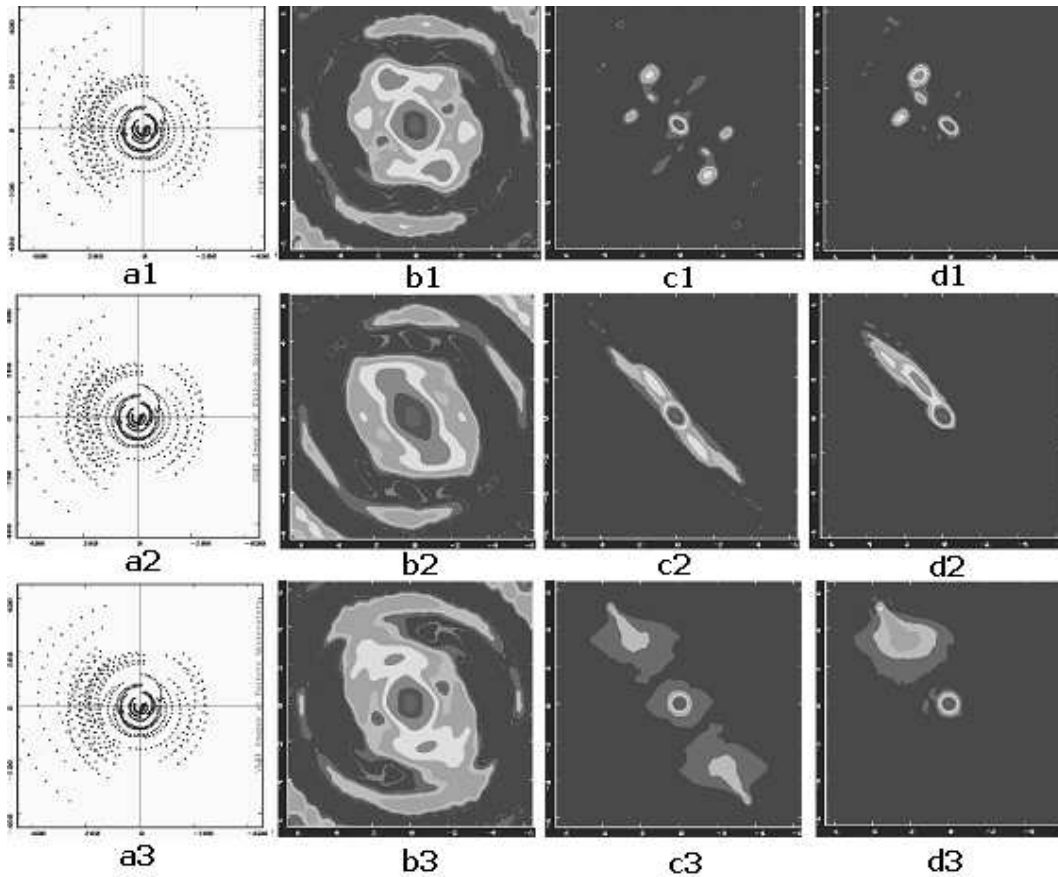


Figure 9: Modelling of "phaseless" mapping in VLBI: columns: (a): UV coverage, (b): "dirty" images, (c): reconstructed intermediate GMEM images with zero-valued spectral phase, (d): Fienup's algorithm output images; rows: (1) for source-1, (2) for source-2, (3) for source-4

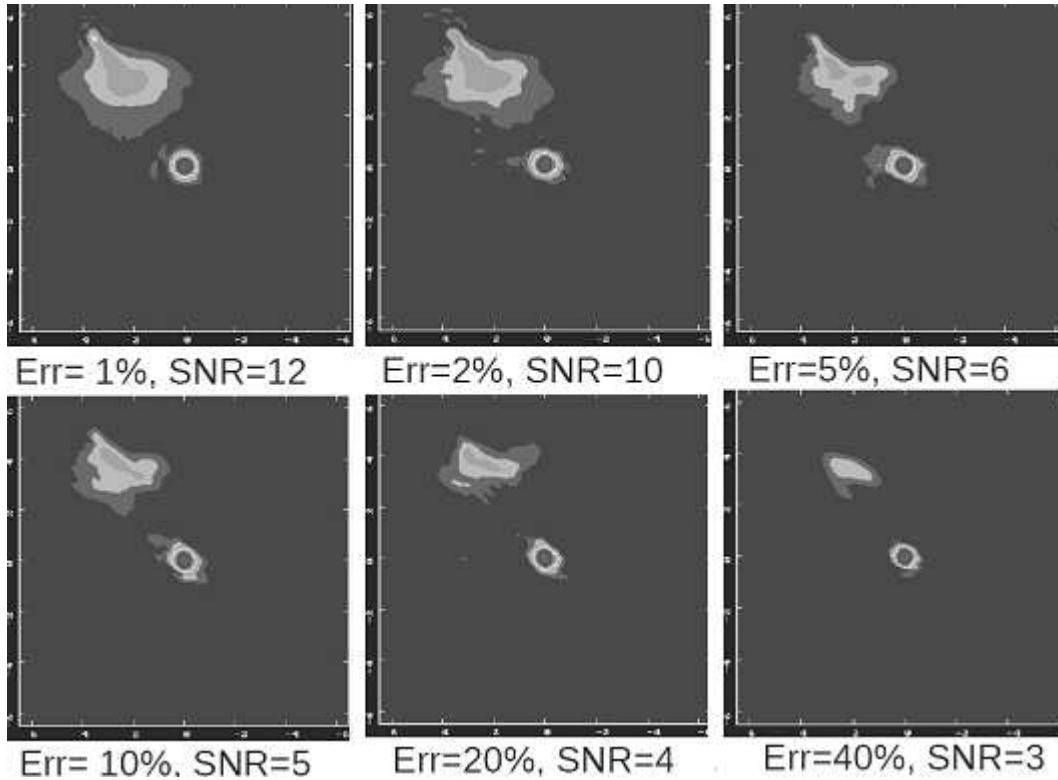


Figure 10: Image reconstruction quality vs visibility magnitude errors for source-4

ters (http://~www.asc.rssi.ru/radioastron/description/orbit_eng.htm) are presented in Fig.18.

In this case, a multi-element interferometer essentially degenerates into a two-element interferometer (Fig.19(a)). The degeneracy of the close-phase relations prevents the use of standard methods for hybrid mapping and self-calibration for the correct reconstruction of images. We suggest that our "phaseless" mapping approach based on methods for the reconstruction of images from only visibility magnitudes (in the complete absence of phase information) can be used in order to achieve the highest resolution of the system.

In Fig.19(b-c) results of modelling of the "phaseless" mapping of compact radio source having weak jet component is shown. Nevertheless the UV coverage of the system is very poor (see Fig.19(a)) the main featured of the source structure were recovered.

8 Conclusions

1. AGNs with structure "bright core + weak jet" are quite suitable objects for "phaseless" VLBI mapping based on standard reconstruction procedures (MEM or CLEAN for deconvolution and Fienup's iterative algorithm for phase retrieval).

2. "Phaseless" mapping is urgent for "RadioAstron" mission because of degenerate closure phases. In order to realize the highest resolution ensured by high-orbit space-ground radio interferometer, it is necessary to use methods for retrieving phase information directly from visibility magnitude measurements.

Acknowledgments

This work was supported by the "Nonstationary Phenomena in Objects of the Universe" Program of the Presidium of the Russian Academy of Sciences and by the "Multiwavelength Astrophysical Research" grant no. NSh-16245.2012.2 from the President of the Russian Federation.

REFERENCES

- A.T. Bajkova, *Astron. Astrophys. Trans.* 1, 313 (1992)
A.T. Bajkova, *Astronomy Letters*, 30, 218 (2004)
A.T. Bajkova, *Astronomy Reports*, 49, 973 (2005)
Yu.M. Bruck and L.G. Sodin, *Optics Comm.*, 30, 304 (1979)
T.J. Cornwell, R. Braun, and D.S. Briggs, in *Synthesis Imaging in Radio Astronomy II. A Collection of Lectures from the Sixth NRAO/NMIMT Synthesis Imaging Summer School*, Ed. by G. B. Taylor, C. L. Carilli, and R. A. Perley (Astron. Soc. Pac., San Francisco, 1999); *Astron. Soc. Pac. Conf. Ser.*, 180, 151 (1999).
J.C. Dainty, and M.A. Fiddy, *Optica Acta*, 31, 325 (1984)
J.R. Fienup, *Opt.Lett.*, 3, 27 (1978)
J.R. Fienup, *Applied Optics*, 21, 2758 (1982)
J.R. Fienup, T.R. Crimmins, and W. Holsztynski, *JOSA*, 72, 610 (1982)
J.R. Fienup, *JOSA*, 73, 1421 (1983)
J.R. Fienup et al., General Dynamics Distinguished Lecture Series, February 9, 2006
J.R. Fienup et al., Workshop on X-ray Science at the Femtosecond to Attosecond Frontier, UCLA, May 19, 2009
B.R. Frieden and A.T. Bajkova, *Appl. Opt.*, 33, 219 (1994)
R. Gerchberg and W.O. Saxton, *Optik*, 35, 237 (1972)
M.H. Hayes, *IEEE Trans. Acoust., Speech, Signal Process.*, 30, 140 (1982)
N.S. Kardashev, *Exp. Astron.*, 7, 329 (1997)
Ya.I. Khurgin and V.P. Yakovlev, *Finite Functions in Physics and Engineering* (Nauka, Moscow, 1971) [in Russian].
A.V. Oppenheim and J.S. Lim, *Proc. IEEE*, 69, 529 (1981)
J.L.C. Sanz and T.S. Huang, *JOSA*, 73, 1442 (1983)
Image Recovery. Theory and Application, Ed. by H. Stark (Academic, Orlando, 1987; Mir, Moscow, 1992)

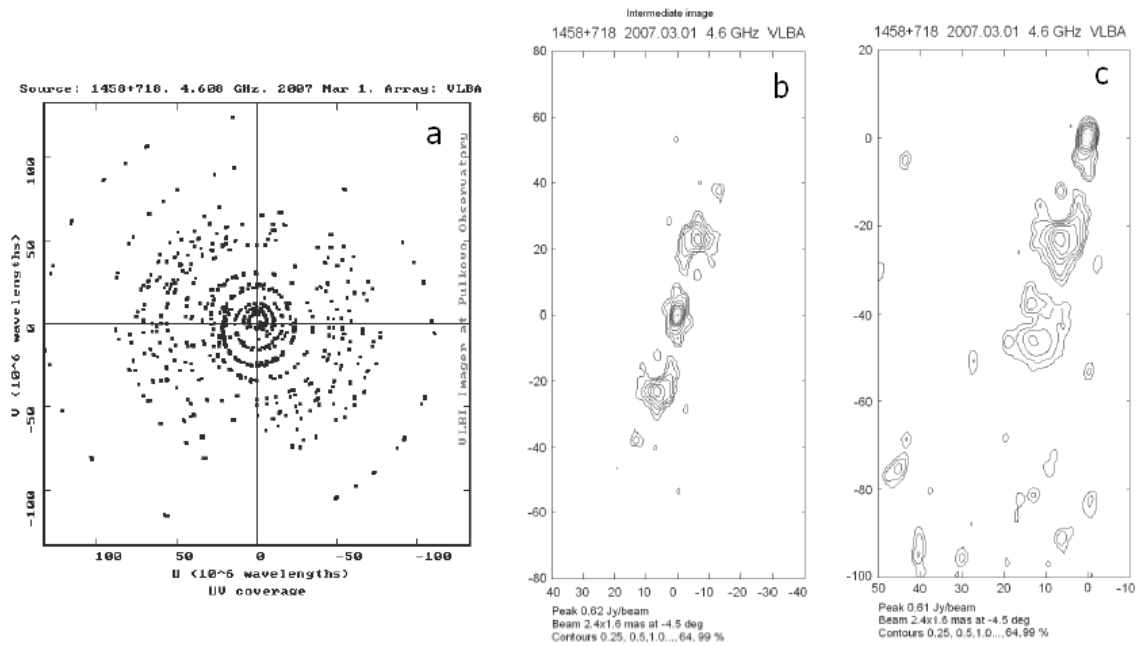


Figure 11: "Phaseless" mapping of 1458+718. (a) UV coverage, (b) reconstructed intermediate GMEM image with zero-valued spectral phase, (c) Fienup's algorithm output image - solution of phase retrieval problem

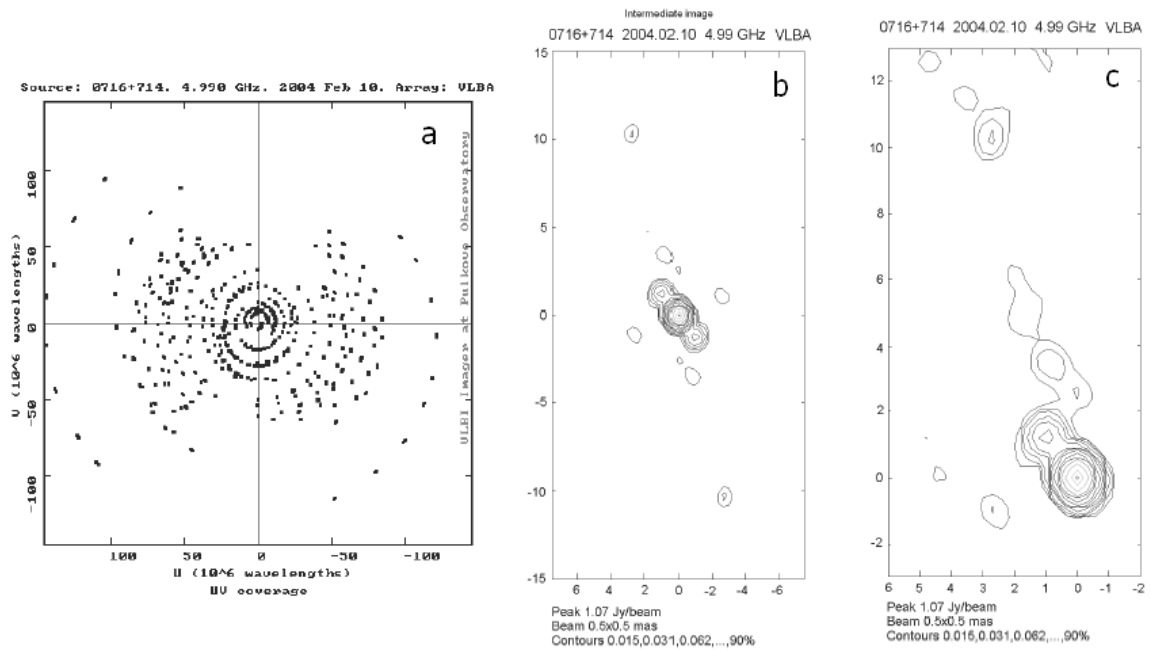


Figure 12: "Phaseless" mapping of 0716+714. (a) UV coverage, (b) reconstructed intermediate GMEM image with zero-valued spectral phase, (c) Fienup's algorithm output image - solution of phase retrieval problem

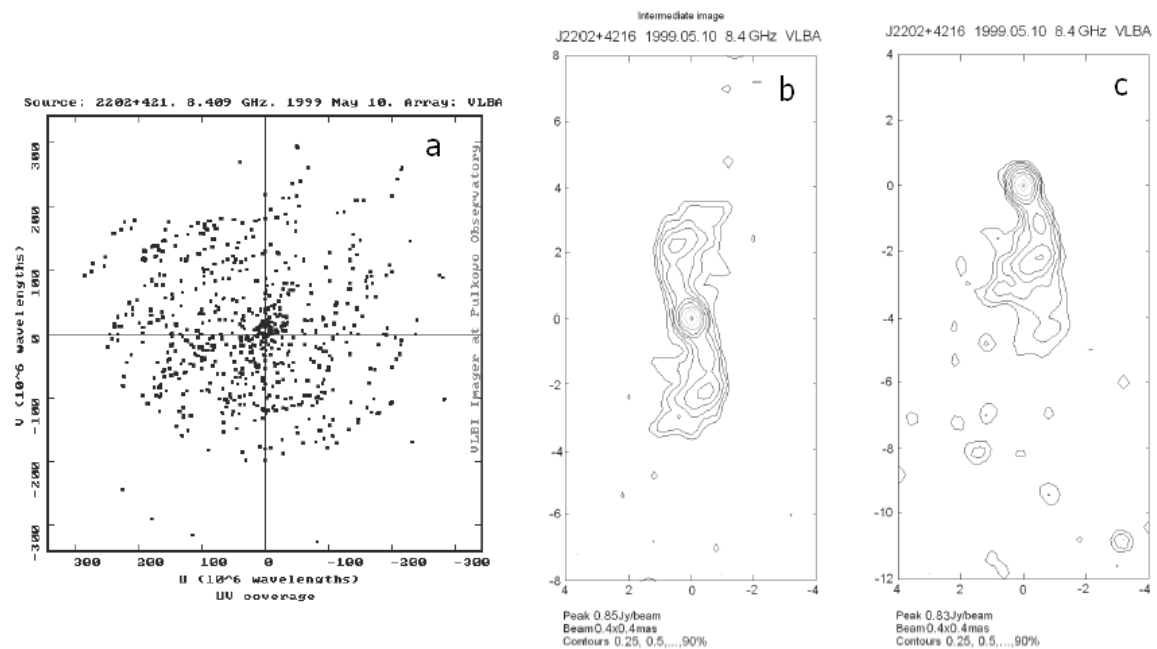


Figure 13: "Phaseless" mapping of J2202+421. (a) UV coverage, (b) reconstructed intermediate GMEM image with zero-valued spectral phase, (c) Fienup's algorithm output image - solution of phase retrieval problem

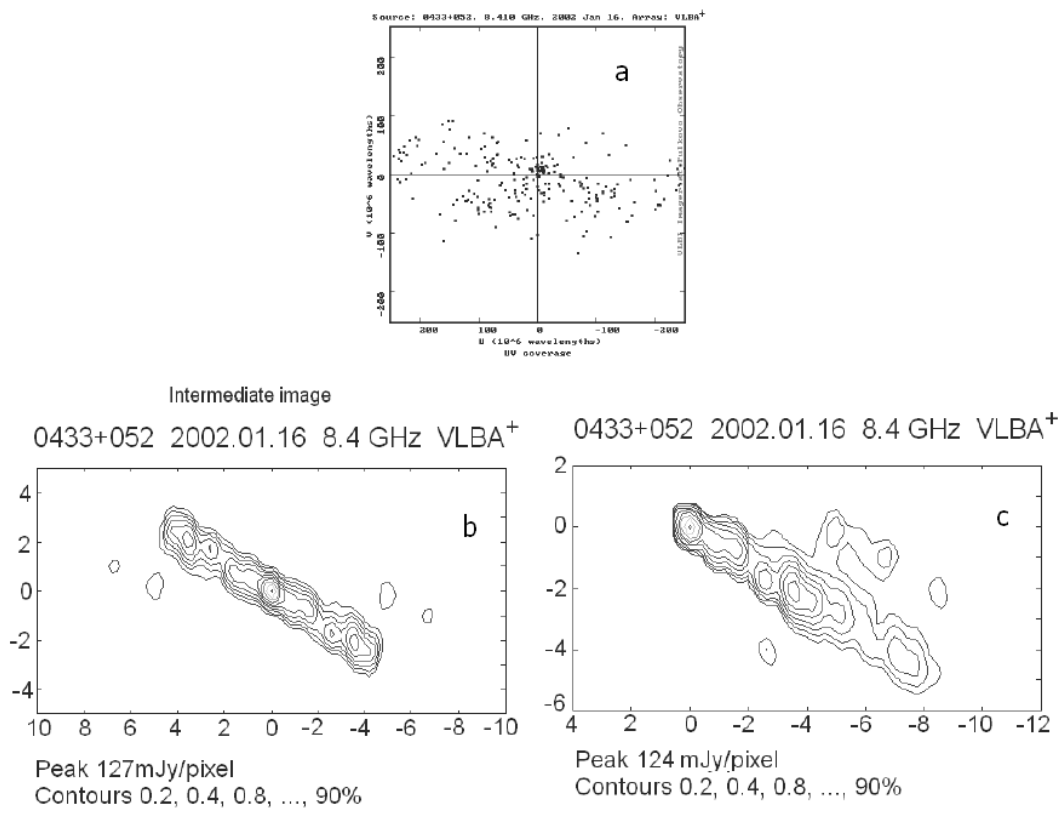
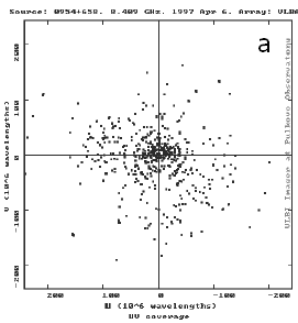
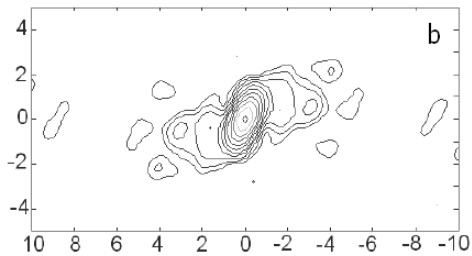


Figure 14: "Phaseless" mapping of 0433+052. (a) UV coverage, (b) reconstructed intermediate GMEM image with zero-valued spectral phase, (c) Fienup's algorithm output image - solution of phase retrieval problem



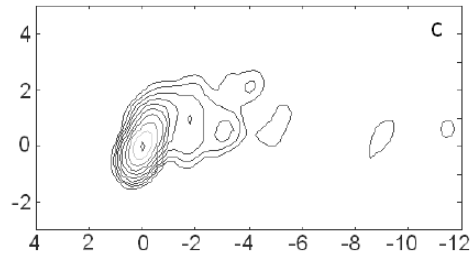
Intermediate image

0954+658 1997.04.16 8.4 GHz VLBA



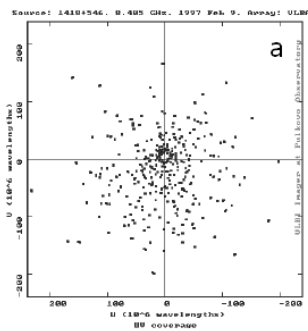
Peak 0.243 Jy/beam
 Beam 0.8x0.6 mas at -16 deg
 Contours 0.1, 0.2, 0.4, ..., 90%

0954+658 1997.04.16 8.4 GHz VLBA



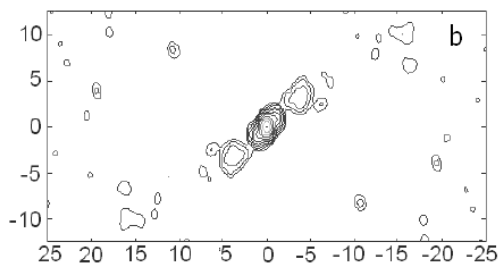
Peak 0.243 Jy/beam
 Beam 0.8x0.6 mas at -16 deg
 Contours 0.2, 0.4, ..., 90%

Figure 15: "Phaseless" mapping of 0954+658. (a) *UV* coverage, (b) reconstructed intermediate GMEM image with zero-valued spectral phase, (c) Fienup's algorithm output image - solution of phase retrieval problem



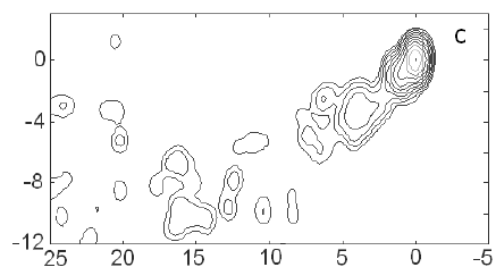
Intermediate image

J1419+4216 1997.02.09 8.4 GHz VLBA



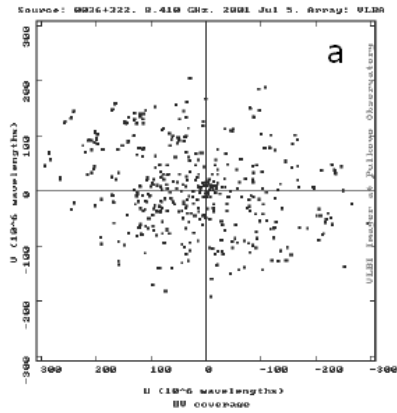
Peak 0.576 Jy/beam
 Beam 1.3x0.8 mas at 0 deg
 Contours 0.1, 0.2, 0.4,..., 99%

J1419+4216 1997.02.09 8.4 GHz VLBA

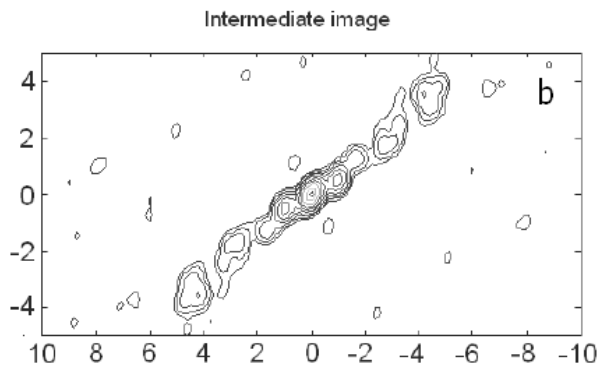


Peak 0.576 Jy/beam
 Beam 1.3x0.8 mas at 0 deg
 Contours 0.1, 0.2, 0.4,..., 99%

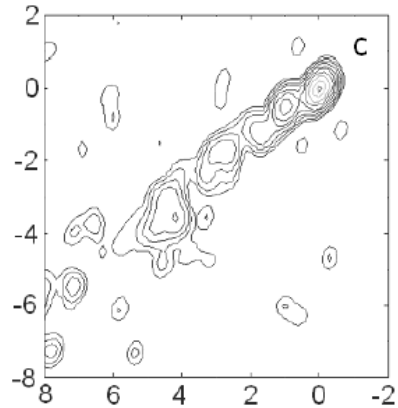
Figure 16: "Phaseless" mapping of J1419+4216. (a) UV coverage, (b) reconstructed intermediate GMEM image with zero-valued spectral phase, (c) Fienup's algorithm output image - solution of phase retrieval problem



J0336+3218 2001.07.05 8.4 GHz VLBA



Peak 0.6 Jy/beam
 Beam 0.5x0.35 mas at -13 deg
 Contours 0.25, 0.5, ..., 90%



Peak 0.59 Jy/beam
 Beam 0.5x0.35 mas at -13 deg
 Contours 0.25, 0.5, ..., 90%

Figure 17: "Phaseless" mapping of J0336+3218. (a) *UV* coverage, (b) reconstructed intermediate GMEM image with zero-valued spectral phase, (c) Fienup's algorithm output image - solution of phase retrieval problem

Perigee radius: $\geq 10,000$ km
 Initial inclination: 51.6°
 Average apogee radius: 350,000 km
 Average period of revolution: 9.5 d

Band	P	L	C	K
Frequencies (MHz) of observations	327	1665	4830	18392-25112
Bandwidth (MHz) for each polarization	4	32	32	32
Fringe size (μ as) [base line 350 000 km]	540	106	37	7,1 -10
Min. cor. flux (mJy) [RMS with EVLA, 300 s integration time]	10	1,3	1,4	3,2

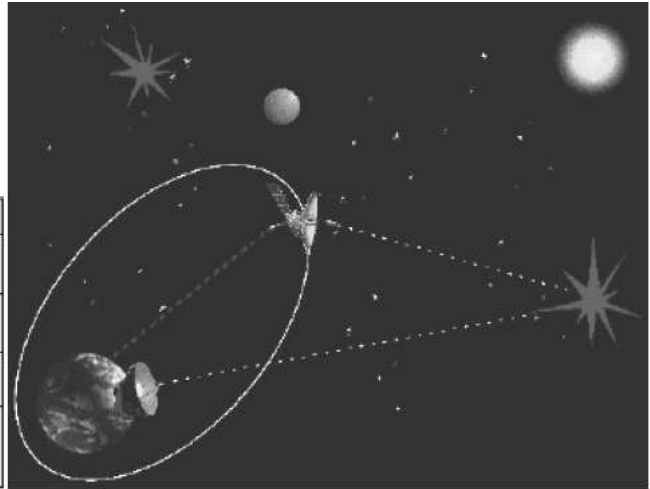


Figure 18: Parameters of Space-Ground Radio Interferometer "RadioAstron"

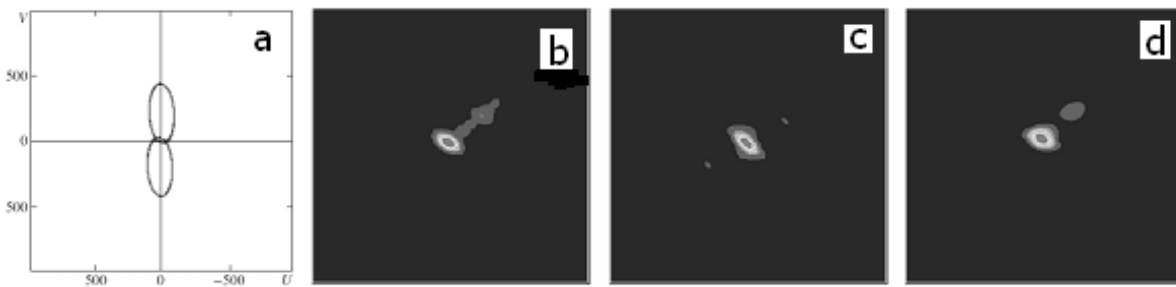


Figure 19: Modelling of "phaseless" imaging in "RadioAstron" system: (a) UV coverage (the scales along the axes are in units of 10^8 wavelengths), (b) model source, (c) reconstructed intermediate GMEM image with zero-valued spectral phase, (d) Fienup's algorithm output image - solution of phase retrieval problem